THE ASTROPHYSICAL JOURNAL, 542:L155–L159, 2000 October 20

COMPOSITIONAL VARIATION ON THE SURFACE OF CENTAUR 8405 ASBOLUS[1]

S. D. KERN,[2] D. W. MCCARTHY,[2] M. W. BUIE,[3] R. H. BROWN,[2,4] H. CAMPINS,[4,5] AND M. RIEKE[2]

Received 2000 June 16; accepted 2000 August 15; published 2000 September 27

ABSTRACT

Near-infrared 1–2 μm spectra of the Centaur 8405 Asbolus (1995 GO) have been obtained using the *Hubble Space Telescope* near-infrared camera and multiobject spectrometer. Strong and variable absorption features indicate a significantly inhomogeneous surface characterized by water ice mixed with additional unknown constituents. Over a 1.7 hr interval, the observed spectra varied from a nearly featureless spectrum to a very complicated absorption spectrum, and the integrated flux varied in a manner consistent with previous light-curve observations. The accepted rotation period of 8.9351 hr assumes a shape-dominated light curve. Our observations indicate that the light curve may in fact be dominated by a relatively bright spot with a period of 4.47 hr, i.e., half the previous value.

Subject headings: infrared: solar system — Kuiper Belt, Oort Cloud

1. INTRODUCTION

Centaurs are small bodies, similar to asteroids, that are believed to have originated in the Kuiper Belt but that currently reside between the orbits of Jupiter and Neptune. The surface compositions of Centaurs and Trans-Neptunian Objects contain clues to the early evolutionary processes operating at large heliocentric distances in the solar nebula. These distant objects are intrinsically faint (V = 19–24) and difficult to study spectroscopically. To date, approximate surface compositions have been estimated from visible and near-infrared wavelengths with broadband photometry and low-resolution spectroscopy (Brown et al. 1998; Brown 2000; Luu & Jewitt 1998; Tegler & Romanishin 1998). In particular, Centaur 5145 Pholus exhibits a mixture of water ice, frozen methanol, organic tholins, and olivine, indicative of a primitive object relatively unprocessed by solar radiation (Cruickshank et al. 1998). Pholus and other such objects exhibit light curves that can be explained by the rotation of an aspherical object and/or by bright surface features. A more in-depth summary of the current understanding of the physical characteristics of these distant objects is presented by Davies (2000).

Using the grism spectroscopy that is available with the near-infrared camera and multiobject spectrometer (NICMOS; Thompson et al. 1998) on board the *Hubble Space Telescope* (*HST*), we have obtained low-resolution 1–2 μm spectra of 8405 Asbolus (1995 GO). NICMOS provides sensitivity comparable to the best ground-based instrumentation and avoids telluric absorptions at 1.4 and 1.9 μm that can partially obscure important absorption features such as water ice.

The 1–2 μm spectra of 8405 Asbolus show its surface to be dramatically inhomogeneous, with one position exhibiting unusually strong absorptions of water ice in combination with a red continuum and other unidentified surface constituents. The strong time dependence of the spectral features suggests that the light curve (Brown & Luu 1997; Davies et al. 1998) may be affected by a bright surface spot of geologically recent origin.

2. OBSERVATIONS

The object 8405 Asbolus was observed during the NIC3 focus campaign on 1998 June 11, at a geocentric distance, heliocentric distance, and phase angle of 9.33 AU, 10.02 AU, and 4°.5, respectively. Low-resolution ($\lambda/\delta\lambda \sim 200$) spectra utilized the G141 (1–2 μm) grism at three different dither positions on the detector array. The dither pattern was a three-position spiral with an amplitude of 20.8 pixels (4″.16) and was chosen to alleviate variations in detector performance along the spectral direction. Three 224 s exposures were obtained in each dither position over a 2 hr time period divided into two sets. The first two positions ("early") were obtained between 14:24:32 and 14:45:01 UT during the first visibility window (orbit), while the third position ("late") images were obtained 1.2 hr later during a second orbit. All the observations used the same guide star.

Direct images with 32 s exposures were taken through the broadband F150W filter in order to assist in the wavelength calibration. These images, obtained between 16:10:15 and 16:13:29 UT, show no evidence of extended structure, although the pixels (0″.2) undersample the point-spread function (PSF).

3. DATA REDUCTION

Spectra from the NIC3 grism images were extracted with reduction software described in Buie & Grundy (2000). The centroid of the object in the F150W image established the location and wavelength calibration of the spectrum. Prior to extraction, the raw frames from oppositely paired dithers were subtracted in order to remove the sky background, the dark current, and systematic detector artifacts. The resulting frame shows both positive and negative spectra of all sources in the field of view. This frame was then flat-fielded with a composite flat field, computed from narrowband flat-field images and the wavelength of illumination at each pixel in the image. Additionally, a small correction for the pixel-response function was applied.

To extract spectra from these calibrated frames, we first created a master PSF for the object by averaging spatial cuts across the spectrum from 1 to 2 μm. The center line of the spectrum was then determined from an iterative process that aligned this

[1] Based on observations with the NASA/ESA *Hubble Space Telescope* obtained at the Space Telescope Science Institute, which is operated by the Association of Universities for Research in Astronomy, Inc., under NASA contract NAS5-26555.

[2] Steward Observatory, University of Arizona, 933 North Cherry Avenue, Tucson, AZ 85721-0065; susank@as.arizona.edu, mccarthy@as.arizona.edu, mrieke@as.arizona.edu.

[3] Lowell Observatory, 1400 West Mars Hill Road, Flagstaff, AZ 86001; buie@lowell.edu.

[4] Lunar and Planetary Laboratory, University of Arizona, Space Sciences Building, P.O. Box 210092, Tucson, AZ 85721-0092; rhb@lpl.arizona.edu, campins@lpl.arizona.edu.

[5] Research Corporation, 101 North Wilmot Road, Suite 250, Tucson, AZ 85711.

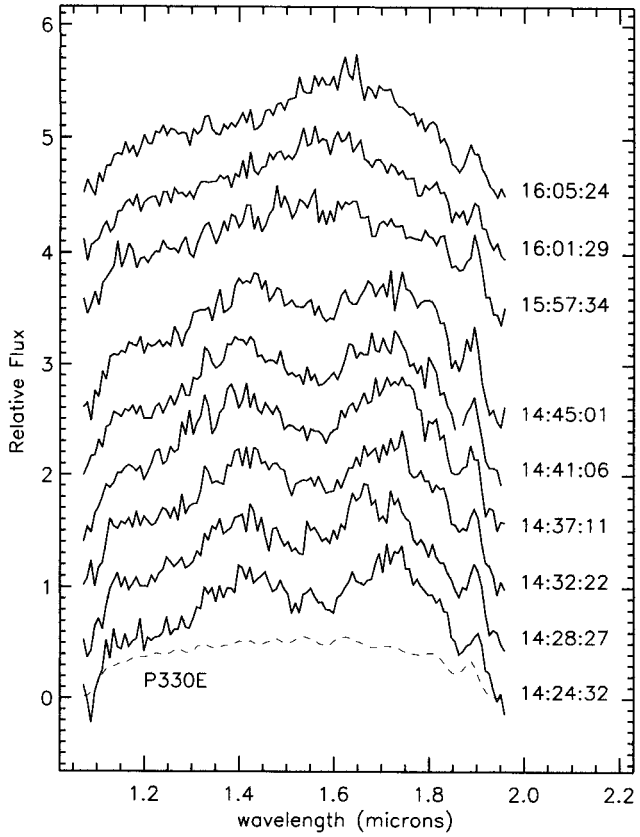

FIG. 1.—Individual raw spectral extractions of 8405 Asbolus. The UT time of each observation is listed to the right of each curve. The lowest spectrum is plotted on an absolute flux scale in millijanskys; the spectra above it are offset vertically by 0.5 mJy with an additional 0.5 mJy between the sixth and seventh spectra to separate the early from the late sequences. The dashed curve at the bottom is the G141 spectrum of the solar-type star P330E observed by NICMOS and multiplied by 0.0025.

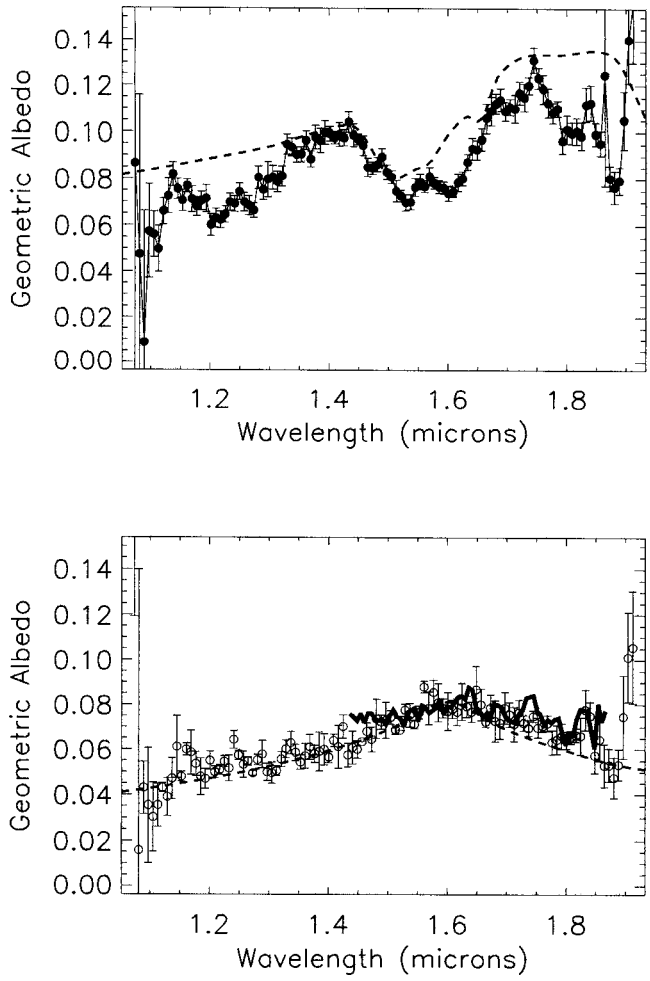

FIG. 2.—*HST*/NICMOS reflectance spectra of the Centaur 8405 Asbolus. The top and bottom panels display the early and late spectra as filled and open circles, respectively. Each spectrum is an average of three to six independent spectra and is normalized by the NICMOS spectrum of the solar-type star P330E. In the bottom plot, a ground-based spectrum (Brown 2000) is superposed for comparison. In each panel, a dashed curve displays a representative model spectrum using a synthetic dark component and, in the early spectrum, water ice. The model spectra are normalized to the geometric albedo at 1.5 μm.

PSF to the spectrum and minimized the residuals. Given a good center line and PSF, the spectrum was extracted using an optimal extraction summation patterned after Horne (1986). At all stages of the iterative spectral extraction, the "goodness" of the extraction was monitored by the internal consistency of the spectra obtained from different observations within the same dither position. Figure 1 shows the time sequence of raw spectra. These spectra are insensitive to changes in the extraction parameters (e.g., PSF, center line, number of iterations).

To convert these spectra into relative reflectance, they have been normalized by the G141 spectrum of a solar-type star, P330E (G0 V; $H = 11.48$; Persson et al. 1998). This star was observed in two separate NICMOS observing programs (GO-7696/7959; Colina & Bohlin 1997). The spectral energy distribution of P330E is the same as the solar reference spectrum to within 2%–3% (Colina & Bohlin 1997). Spectra from six separate dithered observations of this star were extracted in an identical manner and averaged to produce a final reference spectrum. For comparison, we have also extracted the spectrum of a second solar-type star, P035R (G2 V; $H = 10.55$; GO-7055). The spectra of these two stars are the same to within $\lesssim$10%.

The top and bottom panels of Figure 2 show the geometric albedo of 8405 Asbolus both early and late, respectively, after taking the ratio of the observed spectrum of P330E and assuming a 40 km radius. A broad absorption feature between 1.4 and 1.7 μm is visible in the early spectrum with a significant peak just short of 1.6 μm. Other significant absorptions occur at 1.2 μm and longward of 1.8 μm. The narrow spike near 1.84 μm also appears in the star and is not real. Contrary to the early spectrum, the late spectrum shows no significant dips or hints of the absorption edges near 1.4 and 1.7 μm. The slope from 1.2 to 1.6 μm is similar to that of the early spectrum. However, the late spectrum turns over near 1.65 μm and slopes down to the cutoff at 1.85 μm.

4. DISCUSSION

4.1. *Surface Composition*

The spectrum of 8405 Asbolus indicates a complex surface chemistry. The early spectrum shows a deep (~30%) absorption from 1.4 to 1.6 μm. We interpret the absorption edge at 1.45 μm to indicate the presence of water ice that has been detected in weaker strengths on Centaurs 10199 Chariklo (1997 CU26; Brown et al. 1998) and 2060 Chiron (Foster et al. 1999). Since the spectrum in this region is not well reproduced by a

pure water ice model, as shown in the top panel of Figure 2, other absorbers must also be present. These absorbers could also help explain the low value of the measured geometric albedo. A different absorption at 1.2 μm is also unidentified at this time. In sharp contrast, the late spectrum (Fig. 2, *bottom*) lacks these absorption features and displays a sharp turnover near 1.65 μm. This spectrum is in excellent agreement with a recent ground-based spectrum (Brown 2000).

Model spectra were fitted to the data using the Hapke bidirectional reflectance theory (Hapke 1993) and the known optical constants of water ice. The optical constants in our model are taken from Grundy & Schmitt (1998) and Warren (1986). These constants refer to crystalline water ice, measured at temperatures appropriate to 8405 Asbolus, and represent the primary water ice component in our reflectance models. We also include a contribution from an intimately mixed component of water ice whose optical constants are those reported by Warren (1986). Warren's measurements, although strictly applicable at much higher temperatures than thought to exist on Asbolus, provide a closer approximation to the optical constants of amorphous water ice. We chose this approach in order to include a contribution from an amorphous-like water ice component in our models, but we did not have access to the optical constants of amorphous water ice at the appropriate temperature or in the appropriate wavelength region. In addition, to provide a better approximation to the optical constants of amorphous water ice, we shifted the wavelength scale of the Warren (1986) data to agree with the known central wavelengths of the 1.5 and 2.0 μm bands of low-temperature amorphous water ice.

The models also contain a contribution from a simulated dark component. For the early spectrum of 8405 Asbolus, which shows the water ice absorption, a synthetic component was constructed from 15 μm grains with reflectance increasing roughly linearly from about 8% to 20% over the wavelength range of 1–1.7 μm. From 1.7 to 2.0 μm, its reflectance is roughly flat. Such a component with water ice in an intimate mixture produces a model spectrum that matches both the width and the depth of the water ice band and the red continuum of 8405 Asbolus. Certainly this model is not unique but demonstrates one possible way to produce a spectrum that is a reasonable match to one aspect angle of 8405 Asbolus.

The synthetic dark component included in the model calculations was meant to approximate the effect of a very red organic material in an intimate mixture with the water ice. Although it bears a loose spectral resemblance to organic solids produced by the photolysis and radiolysis of mixtures of simple molecular gases (Sagan, Khare, & Lewis 1984), it mainly serves to provide the steep red continuum reflectance displayed by 8405 Asbolus. Similarly, another synthetic dark component with 15 μm grains yields a reasonable match to the reflectance of the late spectral observation of 8405 Asbolus. It is interesting to note that the reflectance of the dark component required to produce an acceptable match is quite different for each of the two aspects observed. This suggests that whatever is reddening the spectrum on the side of 8405 Asbolus where the water ice "spot" is located is of a somewhat different composition than the material on the other face.

We have compared the nine independent spectra in order to look for time-dependent changes. There are possible variations in the spectral shape during the early observations at the 3%–5% level, especially in the depth of the water ice band at 1.55 μm and in the slope from 1.2 to 1.4 μm. We do not, however, observe a gradual transition between the early and late spectra. Observations over a full light curve are necessary to map this transition properly.

4.2. *Light Curve*

The light curve of 8405 Asbolus was first observed by Brown & Luu (1997) and later refined by Davies et al. (1998), who quote an amplitude of 0.55 mag in the R band and a period of 8.9351 ± 0.0003 hr. From the integrated flux versus wavelength in the two NICMOS spectra (Fig. 2), we derive a lower limit to the amplitude at 1.5 μm of 0.33 mag. Davies et al. (1998) base the period determination on the assumption that the object is triaxial. Alternatively, the object could be spherical, and the light curve could be caused solely by albedo variations, as is indicated by the strong spectral variation recorded in the NICMOS spectra. For example, as the object rotates, a single high albedo spot superposed on an otherwise low albedo surface could modulate the reflected light. Such a spot model is described in the following section. If correct, this interpretation would require a rotation period equal to half the above value, 4.47 hr. The high degree of symmetry in the R-band light curve supports this possibility.

The ground-based spectrum obtained by Brown (2000) is in excellent agreement with our late spectrum. However, based on the 8.9351 hr rotation period and the epoch of zero phase (Davies et al. 1998), the former should instead correspond to our early spectrum. The observation by Brown should have occurred at a phase of 0.028 in the light curve compared with the phases for our early (0.007–0.036) and late (0.180–0.195) spectra. With this period, only 258 rotations of 8405 Asbolus occurred between the NICMOS and ground-based epochs. Over this interval, the formal error in period would have accumulated to yield an error of 0.0087 in phase, enough to offset the phase of the ground-based spectrum beyond the final phase of the early NICMOS spectra. These two observations might then sample different surface regions. If the rotation period were half the above value with the same formal error, then the accumulated error in phase is correspondingly larger and can more easily explain the discrepancy.

4.3. *Spot Model*

A surface model incorporating a bright spot superposed on a darker surface can be developed based on the measured flux, light-curve amplitude, and geometric albedos. Although this model is not unique, it is consistent with available data and provides a working hypothesis. We assume that the spot is constrained within a 90° range in longitude and that the surrounding surface is characterized by the late spectrum shown in the bottom panel of Figure 2. Under these conditions, the spot albedo must be $\geq$11% to explain the 0.33 mag variation in observed flux if 8405 Asbolus is spherical in shape. For example, if the spot subtends 1 radian in longitude (6.3% of the total surface area), then its albedo is ~17% and the background surface contributes 75% of the flux in the early spectrum. If we then subtract this background component from the early spectrum, the remaining spectrum is one possible model for the spot as shown in Figure 3.

The background component is not spectrally neutral, as seen in the bottom panel of Figure 2. Removing this component (a real mixture assumed) leaves behind a terrain with an ice and dark material mixture. The resulting spectrum looks more similar to water ice than before the subtraction, but the resulting material is still not a perfect match. The 1.3 μm water band

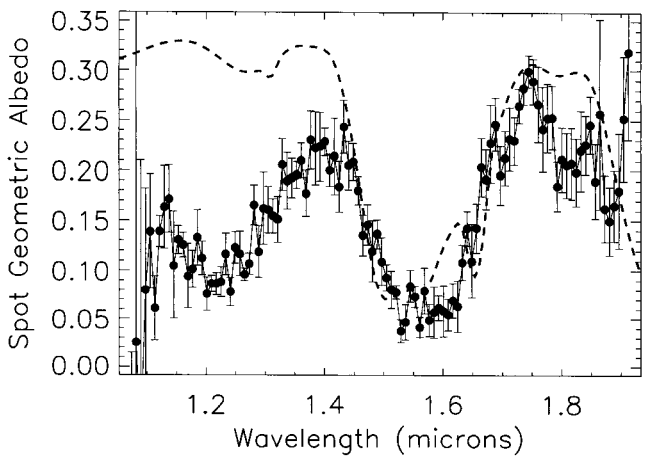

FIG. 3.—Isolated spectrum of the bright terrain on 8405 Asbolus. The data (*filled circles with error bars*) come from subtracting the dark terrain spectrum from the hemisphere with the bright spot (see text for details). The dashed line is one simple model comprised of a mix of crystalline water ice with the same dark material used in the model for the original spectrum of the "spotted" side of 8405 Asbolus. The parameters are 1% dark material with 10 μm grains and 99% water ice with 300 μm grains. The water ice component is modeled by optical constants at 60 K from Grundy & Schmitt (1998).

does not appear in our spectrum, and the 1.5 μm band is too low at 1.6 μm. This spot spectrum reveals a spectral signature and a mix of materials that have not been seen until now. Our data set is insufficient to provide a full understanding of the surface. Clearly, a more intensive set of spectral measurements is needed over an 8–10 hr period.

Although the light curve of 8405 Asbolus may be caused entirely by a single high albedo surface feature, a combination of albedo variations and a nonspherical shape provides a more likely explanation. An icy object in the Centaur region should have a radius of at least 200 km in order to deform into an equilibrium shape (Slyuta & Voropaev 1997). Based on the average flux, i.e., 0.45 mJy measured in these NICMOS spectra, and an assumed albedo of 0.07, the radius of 8405 Asbolus is about 40 km.

4.4. *V−R Color Measurements*

Previous authors have reported apparently discrepant $V-R$ colors of 8405 Asbolus. The high values of 0.68 and 0.78 reported by Brown & Luu (1997) may in fact be consistent with the lower values of 0.4–0.5 measured by Romanishin & Tegler (1997) and Davies et al. (1998) if different surface areas were observed. For example, since both $V-R$ observations were obtained at nearly the same epoch (1996 April 14–17), the light curve established by Davies et al. (1998) can be used with sufficient precision to show that these observations refer to different locations on 8405 Asbolus. The redder color measured by Brown & Luu may conceivably characterize the same region observed in the NICMOS spectra. However, if the rotational period is shorter (i.e., 4.47 hr), the $V-R$ measurements overlap in rotational phase and would be discrepant.

4.5. *Implications*

The known populations of Centaur and Kuiper Belt objects display a wide range of surface colors and compositions. Some of this diversity may be attributed to the production of "irradiation mantles" produced by the interaction of solar ultraviolet light, ions, and/or cosmic rays with carbon-bearing ices on the surface. With increasing exposure, an originally icy surface is thought to become redder and darker as a layer of carbon compounds accumulates to a depth of ~1 m (Jewitt & Luu 2000). The surface reflectivity may ultimately exhibit a neutral color (Moroz et al. 1998).

The above evolutionary scenario is supported by the spectral diversity within the 8405 Asbolus spectra. An impact event may have penetrated the reddish mantle, exposing the underlying ice. Such an impact may also have generated its potentially rapid rotation rate. Objects like 8405 Asbolus should collide with impactors of radii ~500 m every 10^6–10^7 yr (Stern 1995) without suffering complete disruption (Farinella & Davis 1996).

The above scenario, combined with recent light-curve observations, suggests an evolutionary sequence of known Centaur objects. Centaur object 10199 Chariklo exhibits water ice absorption (Brown et al. 1998) without light-curve modulation (S. D. Kern & R. M. Wagner 2000, in preparation). Thus, its surface may be relatively uniform and young. The spectra of the three Centaurs, 8405 Asbolus, 5145 Pholus, and 2060 Chiron, vary from extremely red to neutral in color, suggesting increasing exposure times to irradiation. This sequence may reflect the order of their entry into the Centaur region. However, the situation is complicated by the known activity of 2060 Chiron and the implication that other Centaurs may show activity as well.

5. CONCLUSIONS

Near-infrared spectroscopy with *HST*/NICMOS has revealed significant surface inhomogeneity on the Centaur 8405 Asbolus. Over 1.7 hr, strong absorption features attributed to water ice and other unidentified species vanish entirely. These observations suggest that the visible light curve may be dominated by albedo variations and that 8405 Asbolus may be rotating faster (4.47 hr) than previously suspected.

Support for this work was provided by NASA through grant GO-07822.01-96A from the Space Telescope Science Institute, which is operated by the Association of Universities for Research in Astronomy, Inc., under NASA contract NAS5-26555. We also acknowledge support from NASA project NAG-53359. The authors are grateful to M. Brown for providing data in advance of publication and to Tony Roman at the Space Telescope Science Institute who coordinated these observations.

REFERENCES

Brown, M. E. 2000, AJ, 119, 977
Brown, R. H., Cruikshank, D. P., Pendleton, Y., & Veeder, G. J. 1998, Science, 280, 1430
Brown, W. R., & Luu, J. X. 1997, Icarus, 126, 218
Buie, M. W., & Grundy, W. M. 2000, Icarus, in press
Colina, L., & Bohlin, R. 1997, AJ, 113, 1138
Cruikshank, D. P., et al. 1998, Icarus, 135, 389
Davies, J. K. 2000, in Proc. ESO Workshop on Minor Bodies of the Outer Solar System (Dordrecht: Kluwer), in press
Davies, J. K., McBride, N., Ellison, S., Green, S., & Ballantyne, D. R. 1998, Icarus, 134, 213
Farinella, P., & Davis, D. R. 1996, Science, 273, 938
Foster, M. J., Green, S. F., McBride, N. & Davies, J. K. 1999, Icarus, 141, 408
Grundy, W. M., & Schmitt, B. 1998, J. Geophys. Res., 103, 25,809
Hapke, B. 1993, in Remote Geochemical Analyses: Elemental and Mineralogical Composition, ed. C. M. Pieters (New York: Cambridge Univ. Press), 31

Horne, K. 1986, PASP, 98, 609
Jewitt, D., & Luu, J. 2000, in Protostars and Planets IV, ed. E. Mannings, A. Boss, & S. Russell (Tucson: Univ. Arizona Press), 1201
Luu, J. X., & Jewitt, D. C. 1998, ApJ, 494, L117
Moroz, L., Arnold, G., Korochantsev, A., & Wasch, R. 1998, Icarus, 134, 253
Persson, S. E., Murphy, D. C., Krzeminski, W., Roth, M., & Rieke, M. J. 1998, AJ, 116, 2475
Romanishin, W., & Tegler, S. C. 1997, AJ, 113, 1893
Sagan, C., Khare, B. N., & Lewis, J. S. 1984, in Saturn, ed. T. Gehrels (Tucson: Univ. Arizona Press), 1139
Slyuta, E. N., & Voropaev, S. A. 1997, Icarus, 129, 401
Stern, S. A. 1995, AJ, 110, 856
Tegler, S. C., & Romanishin, W. 1998, Nature, 392, 49
Thompson, R. I., Rieke, M., Schneider, G., Hines, D. C., & Corbin, M. R. 1998, ApJ, 492, L95
Warren, S. G. 1986, Appl. Opt., 25, 2650